

Context-aware Human Motion Prediction

Enric Corona

Albert Pumarola

Guillem Alenyà

Francesc Moreno

Institut de Robòtica i Informàtica Industrial, CSIC-UPC, Barcelona, Spain
{ecorona, apumarola, galenya, fmoreno}@iri.upc.edu

Abstract

The problem of predicting human motion given a sequence of past observations is at the core of many applications in robotics and computer vision. Current state-of-the-art formulate this problem as a sequence-to-sequence task, in which a historical of 3D skeletons feeds a Recurrent Neural Network (RNN) that predicts future movements, typically in the order of 1 to 2 seconds. However, one aspect that has been obviated so far, is the fact that human motion is inherently driven by interactions with objects and/or other humans in the environment.

In this paper, we explore this scenario using a novel context-aware motion prediction architecture. We use a semantic-graph model where the nodes parameterize the human and objects in the scene and the edges their mutual interactions. These interactions are iteratively learned through a graph attention layer, fed with the past observations, which now include both object and human body motions. Once this semantic graph is learned, we inject it to a standard RNN to predict future movements of the human/s and object/s. We consider two variants of our architecture, either freezing the contextual interactions in the future of updating them. A thorough evaluation in the “Whole-Body Human Motion Database” [21] shows that in both cases, our context-aware networks clearly outperform baselines in which the context information is not considered.

1. Introduction

The ability to predict and anticipate future human motion based on past observations is essential for interacting with other people and the world around us. While this seems a trivial task for a person, it involves multiple sensory modalities and complex semantic understanding of the environment and the relations between all objects in it. Modeling and transferring this kind of knowledge to autonomous agents would have a major impact in many different fields, mainly in human-robot interaction [22] and autonomous driving [37], but also in motion generation for computer

graphics animation [23] or image understanding [5].

The explosion of deep learning, combined with large-scale datasets of human motion such as Human3.6M [16] or the CMU motion capture dataset [25], has led to a significant amount of recent literature that tackles the problem of forecasting 3D human motion from past observations [8, 17, 34, 12, 3, 28, 9]. These algorithms typically formulate the problem as sequence-to-sequence task, in which past observations represented 3D skeleton data are injected to a Recurrent Neural Network (RNN) which then predicts movements in the near future (less than 2 seconds).

Nevertheless, while promising results have been achieved, we argue that the standard definition of the problem used so far lacks an important factor, which is the influence of the rest of the environment on the movement of the person. For instance, if a person is carrying a box, the configuration of the body arms and legs will be highly constrained by the 3D position of that box. Discovering such interrelations between the person and the object/s of the context (or another person he/she is interacting with), and how these interrelations constrain the body motion, is the principal motivation of this paper.

In order to explore this new paradigm, we devise a context-aware motion prediction architecture, that models the interactions between all objects of the scene and the human using a directed semantic graph. The nodes of this graph represent the state of the person and objects (e.g. positional features) and the edges their mutual interactions. These interactions are iteratively learned with the past observations of the human and objects motion and fed into a standard RNN which is then responsible for predicting the future movement of all elements in the scene (for both rigid objects and non-rigid human skeletons). Additionally, we propose a variant of this model that also predicts the evolution of the adjacency matrix representing the interaction between the elements of the scene.

Presumably, one of the reasons why current state-of-the-art has not considered an scenario like ours is because all methods are trained and evaluated on benchmarks (mostly the aforementioned Human3.6M dataset [16]) annotated

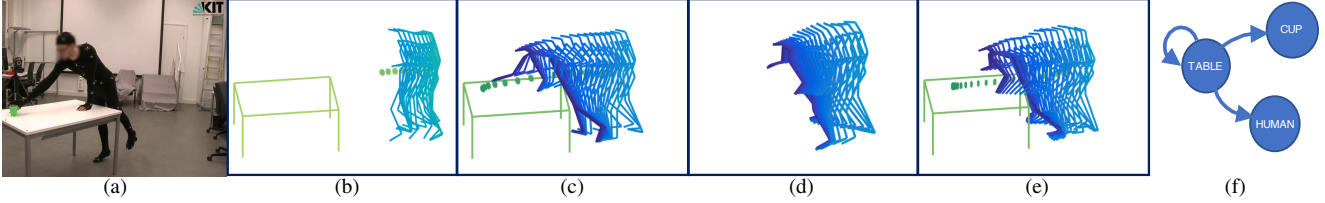


Figure 1: **Context-aware human motion prediction.** (a) Sample image of a sequence with a person placing a cup on a table. Note that this image is shown solely for illustrative purposes. Our approach only relies on positional data. (b) Past observations of all elements of the scene, the person, the cup and the table. (c) Ground truth future movements. (d) Human motion predicted using [34], consisting of an RNN that is agnostic of the context information. Note that there is a large gap with the ground truth, especially for the final frames of the sequence. (e) Cup and human motion prediction obtained with our context-aware model. While the arm of the person is not fully extended, the forecasted motion highly resembles the ground truth. Interestingly, the interaction with the table also helps to set the motion boundaries. (f) Main interactions that are learned with our approach in which dominates the influence of the table over both the cup and the person.

only with human motion. In this paper, we thoroughly evaluate our approach in the “Whole-Body Human Motion Database” [21], that contains about 200 videos of people performing several tasks and interacting with objects. This dataset is annotated with MoCap data for the humans and rigid displacement for the rest of objects, being thus, a perfect benchmark to validate our ideas. The results on this dataset show that our methodology is able to accurately predict the future motion of people and objects while simultaneously learning very coherent interaction relations. Additionally, all context-aware versions, clearly outperform the baselines which uniquely rely on human past observations of the human (see Fig. 1).

2. Related work

Human motion prediction. Since the release of large-scale MoCap datasets [16, 21], there has been a growing interest in the human motion prediction problem. Most approaches build upon RNNs [8, 34, 12, 3] that encode historical motion of the human and predict the future configuration that minimizes different sort of losses. Martinez *et al.* [34], for instance, simply minimize the L2 distance and provide one of the baselines in our work. This work also compares against a zero-velocity baseline, which despite steadily predicting the last observed frame, yields very reasonable results under the L2 metric. This phenomenon has been recently discussed by Ruiz *et al.* [40], that argue that L2 distance is not an appropriate metric to capture the actual distribution of human motion, and that a network trained using only this metric is prone to converge to a mean body pose. To better capture real distributions of human movement, recent approaches use adversarial networks [11, 2] in combination with geometric losses [3, 12, 40, 24].

There exist alternative approaches other than RNNs. For instance, Jain *et al.* [17] consider a hand-crafted spatial-temporal graph adapted to the skeleton shape. Li *et al.* [28]

use Convolutional Neural Networks to encode and decode skeleton sequences instead of RNNs.

All methods described in this section formulate the human prediction problem without considering the context information. In this paper, we aim to fill this gap.

Rigid object motion prediction. There is an immense amount of work on this topic, and here we just mention those which are more related to our approach. Some works aim to predict motion in video without explicitly considering entities or particular objects. For instance, Byeon *et al.* [4] use ConvLSTMs aggregating information from all pixels efficiently for improved video prediction. Other works predict object and human motion in videos via optical flow [42, 31].

The main area of research on this topic is currently focused on car intention prediction for autonomous driving. Some works follow an intuitive approach of taking roads into account and constraining the car movement to be within the expected tracks. For instance, Deo *et al.* [7] classify car motions into a few possible maneuvers on a freeway before predicting trajectories for each car. [30] uses a 3D CNN for car detection, tracking and motion prediction. This work relies on a set of anchor boxes which are very well suited to car shapes and, during detection, they predict the bounding box for the current frame and the following ones. Altché *et al.* [1] propose a more general approach by using an RNN to predict motion from vehicles using features like position, velocity and distance from the ego-car.

Human-Object Interaction (HOI). Even though our work does not aim to identify Human-Object relationships, we have been inspired by a few papers on this topic. The standard formulation of the problem consists in representing an image with several detected objects and people as a graph encoding the context [14, 35, 39, 32, 10], or some other structured representation [27, 45].

The most recent approaches [28, 39, 14] extract features

of the detected entities using some image-based classification CNNs. Then, they compare pairs of features to predict their mutual interaction. Qi *et al.* [39] refine the representations and predicted interactions in a recursive manner. In this work, we use a similar idea to progressively refine the estimation of the interactions between objects.

Graph-based context reasoning. A few works leverage context information to boost the performance of different tasks [38, 29, 15, 26, 36]. Graph Convolutional Networks (GCNs) [19] were recently proposed for improved semi-supervised classification. Jain *et al.* [17] used Structural RNNs to model spatio-temporal graphs. Wang *et al.* [43] propose to use GCNs, in which the interactions between objects depend on the intersection over union of their detected bounding boxes. Chen *et al.* [5] introduce an approach for image segmentation in which features from a 2D image coordinate space are represented in a graph reasoning space.

3. Problem formulation

Recent methods for human motion prediction consist of a model \mathcal{M} , typically a deep neural network, that encodes motion from time t_o until $t - 1$. The goal is then to predict future human motion until t_f , namely $P_{t:t_f}$, where P stands for the human pose represented by 3D joint coordinates. Previous approaches have formulated the problem as $\mathcal{M} : P_{t_o:t-1} \rightarrow P_{t:t_f}$, i.e. future motion is estimated only from past observations. In this paper, we conjecture that future motion is also driven by the context and the action the human is performing. We therefore consider other objects O of type T in the scene with which the human may interact. The objects can be other people or any object in the scene. We will design our approach to be able to predict the motion of such objects of the context.

Additionally, the influence that objects will have in the future motion of other objects is unclear. Thus, we also aim to build a model that learns these interactions between objects in an unsupervised manner. Considering all this, we reformulate our problem as the estimation of the following mapping:

$$\mathcal{M} : \{P_{t_o:t-1}, O_{t_o:t-1}, T\} \rightarrow \{P_{t:t_f}, O_{t:t_f}, I_{t_o:t_f}\}, \quad (1)$$

where I corresponds to the predicted interactions.

4. Approach

Figure 2 introduces the main architecture used in this work. It consists of two branches that separately process human motion and object relationships. We use the latter to obtain a representation for all the observed entities, including the human, which we then use to predict both human and object motion prediction. We next describe the two branches in detail.

4.1. Human motion branch

This branch builds upon the RNN network proposed by Martinez *et al.* [34]. This model, depicted in blue in Figure 2, is based on a residual architecture [13] that, at each step, uses a fully connected layer to predict the velocity of the body joints. As in a typical sequence-to-sequence network, the predictions are fed to the next step.

4.2. Context branch

The context information is represented using a directed graph structure where each node denotes an object or a person. We then store a state for each entity and frame, that encodes context information relevant to each node. These states are iteratively refined as new observations are processed.

Object representation. At each frame t , we define a matrix $X_t \in \mathbb{R}^{N \times F_0} = [O_t, T_t, P_t]$ that gathers the representation of all N nodes. F_0 is the length of the state vector of each node, and contains the object 3D bounding box O_t , their object type T as a one-hot vector, and the joints of the person P_t . If the node does not correspond to a person, the joints in the representation are set to a zero vector of the same size. The object type helps to identify the task the human is performing and the motion defined for that task. By doing this, we aim to capture the semantic difference between the motion of a person when handling a knife or when using a whisk.

Modelling contextual object representations. Recent works on Graph Convolutional Networks (GCNs) [19] have shown very promising results in a variety of problems requiring the manipulation of graph-structured data. In GCNs, a feature vector of a certain node R_i is expressed as a function of other nodes x , as $R_i = \sigma(\sum_j \tilde{A}_{ij} W x_j)$, where W are trainable weights, σ is an activation and N the number of nodes of the graph connected to the i -th node. $\tilde{A} \in \mathbb{R}^{N \times N}$ is a normalized weighted adjacency matrix that defines interactions between nodes.

In this paper, we use Edge Convolutions [44], which are very similar to GCNs. In ECs the update rule for a feature vector of each entity considers the representations of other relevant objects as follows:

$$R_i = \sigma(\sum_j \tilde{A}_{ij} W [x_i; x_i - x_j]). \quad (2)$$

The intuition behind this equation is that x_i encodes a global representation of the node, while $x_i - x_j$ provides local information. EC proposes combining both types of information in an asymmetric graph function.

We keep track of the context representations during all observations through a second RNN. Each node on the

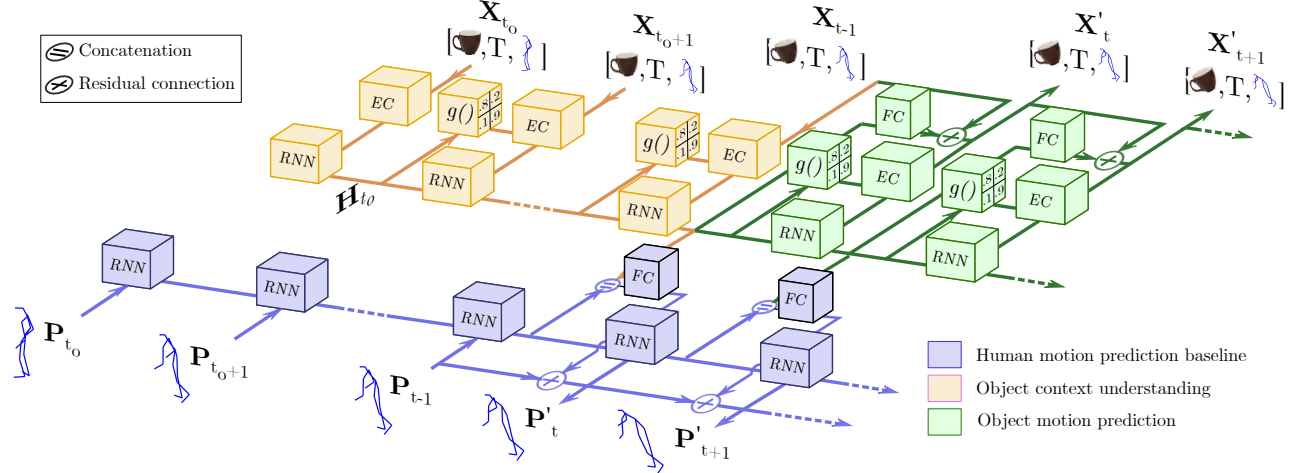


Figure 2: An overview of our context-aware motion prediction model. The blue branch represents a basic RNN that encodes past poses and decodes future human motion using a residual layer [34]. The upper branch corresponds to an RNN that encodes the contextual representation for each object in the scene. This branch contains two modules (depicted in brown and green). In brown, the past object position, class, and human joints are used to predict interactions and context feature vectors. The node corresponding to the human contextual representation is then used in conjunction with the human motion hidden state, to predict human motion. In green, the model is extended to predict motion of all observed objects. Best viewed in color.

scene has a hidden state H that is updated every frame t :

$$H_i^{t+1} = \text{RNN}(R_i^t, H_i^t). \quad (3)$$

Learning interactions. As we shall see in the experimental section, we initially evaluate a simplified version of our Context-RNN (C-RNN) that uses a heuristic to define the adjacency matrices, setting $A_{ij} = 1$ if the center of gravity of objects i and j is closer than 1 meter.

In practice, interactions between entities are not known a priori, and furthermore, they change over time. Our goal is to automatically learn these changing interactions with no supervision. For this purpose we devise an iterative process in which, for the first frame, we set A to a diagonal matrix, *i.e.* $\tilde{A}_{t_0} = I_N$, meaning that the initial hidden representation of every object depends only on itself. We then predict the value of the interaction between two objects given the hidden state of both. We consider asymmetric weighted adjacency matrices, that for a frame t are estimated as:

$$A_{ij}^t = g(H_i^t, H_i^t - H_j^t). \quad (4)$$

This follows the same intuition described in Eq. 2 to combine both global and local structure when predicting the value of the interaction between nodes i and j . The function g represents the output of a neural network layer, in our case a fully connected. We finally use a Softmax function to normalize the interactions for each node i :

$$\tilde{A}_{ij}^t = \frac{\exp(A_{ij}^t)}{\sum_k \exp(A_{ik}^t)}, \quad (5)$$

where N stands for the total number of object in the scene. Note that self-interactions are also included in the diagonal of the adjacency matrix.

Intuitively, we can consider this as a complete graph, where a graph attention mechanism [41] decides on the strength of interactions based on past observations. Note that while existing works typically use binary adjacency matrices from ground truth relationships [19], spatial assumptions [43] or K-Nearest Neighbours on node representations [44], in this work we consider a differentiable continuous space of interactions, which is learned using back-propagation.

In the rest of the paper we will denote the models that learn interactions with the suffix “-LI” (*e.g.* C-RNN+LI).

Object motion prediction. We propose two methods that exploit context at different levels. First, in the blue+brown modules of Figure 2, we consider a model that reasons about the past context observations and iteratively improves hidden representations. The refined context representation of the human node is concatenated to the baseline branch (in blue) representation at every time step, and used by a fully connected layer to predict human velocity in that step. This is followed by a residual layer, that yields skeleton poses.

Our second approach consists of the complete model depicted in Figure 2 which, apart from past context, predicts object motion for all objects using a residual fully connected layer on each object hidden state. Analogous to the human motion branch, the predicted positions are forwarded to the

next step, allowing to extend the context analysis into the future. The joints in the feature representations for those nodes describing people are also updated with the joint predictions of the human branch.

Additionally, when tracking several people, the human motion branch is repeated for each of them, and the model provides complete future motion for all available entities. In the rest of the document, we will denote the models that predict object motion with the suffix “-OPM”.

5. Implementation details

In this section, we elaborate on the architecture of the model and training details.

Architecture. Our model builds on the residual architecture of Martinez *et al.* [34] to allow an unbiased comparison with their work. The recurrent model is based on Gated Recurrent Units (GRUs) [6] followed by a fully connected layer that predicts the change in the human position with respect to the last frame. The recurrent model for context is also based on GRUs. The size of the human and object RNN hidden representations are 1024 and 256, respectively.

We use a similar approach as in [39] to obtain the adjacency matrix. We build a 4D matrix A such that A_{ij} contains the hidden representations $[H_i^t; H_i^t - H_j]$ of nodes i and j , extending over the channel dimension. The function $g(\cdot)$ is formed by two Convolutional Layers of output kernel size 1, to make computation faster. We do not use bias term neither in these Convolutional layers nor in the Edge Convolutions.

For the graph model, we experimented using GCNs [20] and Edge Convolutions [44]. We found GCN-based models not able to learn relevant object interactions and, after convergence, all the interactions had the same strength. In contrast, Edge Convolutions were designed to operate on Cartesian spaces. Since they compare representations of two nodes when computing the representation of the next layer, they have the capacity to compare 3D positions and identify objects that are close. Additionally, we experimented with one and two EC layers. Increasing depth may lead to interesting analysis on the interactions learned, but we noticed our models were prone to overfitting.

The representation of the object is formed first by the bounding box position, defined by the minimum and maximum 3D Cartesian points.

Loss function. We train the model to minimize $L2$ distance between the predicted and the actual future motion $\mathcal{L} = ||M(P_{t_o:t-1}) - P_{t:t_f}||_2$.

Training details. After the motion seed, we sample an observation every 100 ms. In all experiments, we encode and decode 10 (1 sec.) and 20 frames (2 sec.) respectively. Larger encoding times did not help in improving the results and significantly increased training time.

	Passing objects	Grasping/ leaving object	Cutting food	Mixing objects	Cooking	All
# objects	4	5	6	9	12	15
# people	2	1	1	1	1	1/2
# videos	18	36	10	17	35	190
# frames	30k	31k	11k	14k	54k	198k

Table 1: **Dataset statistics.** We train on classes with different number of objects or people to evaluate how the models perform depending on the complexity of the scene. This dataset is a subset of the Whole-Body Human Motion Database [33].

We also do augmentation in the train set through random rotation over the height Z in the range $(-180, 180]^\circ$ and random translation $X, Y \in (-1500, 1500)$ mm. We do not normalize joints respect to center of gravity or any other particular joint, like in [3]. This allows predicting absolute motion. The model is trained until convergence, using Adam [18] with learning rate of 0.0005, beta1 0.5, beta2 0.99 and batch size 16.

6. Experiments¹

Dataset. Large-scale MoCap datasets [21, 16, 25] provide annotations on the human poses but do not give any annotation about objects of the scene or any relevant context information. Therefore, most recent works on human motion prediction are evaluated without considering context information. Martinez *et al.* [34] show that for certain cases, even a simple zero-velocity baseline may yield better results than context-less learning models.

To demonstrate the merits of our approach, we leverage on the Whole-Body Human Motion Database [33], a large-scale publicly available dataset containing 3D raw data of multiple individuals and objects. In particular, we use all the activities where human joints are provided and include at least a table. This results in 190 videos and 198K frames, and a total of 15 tracked object classes. We use the raw recordings Vicon files at 100 Hz to obtain the bounding box of each object in each frame, and select 18 joints to represent the human skeleton.

We extract different actions representing different levels of complexity on the contextual information, summarized in Table 1. We will report results on both action-specific models and also on models trained with the entire dataset. For all the experiments, we split the number of videos into train (60%), validation (20%) and test (20%) sets. The results presented in the rest of the work are obtained from the test set.

Baselines. We compare our models to the context-less models proposed in [34]. First, we consider the basic residual

¹We plan to release the code and data to run all our experiments.

Human motion prediction	Passing objects				Grasping or leaving object				Cutting food				Mixing objects				Cooking			
Time (s)	0.5	1	1.5	2	0.5	1	1.5	2	0.5	1	1.5	2	0.5	1	1.5	2	0.5	1	1.5	2
ZV [34]	34	81	120	153	89	222	333	421	54	132	198	258	102	262	396	495	24	53	70	80
RNN [34]	50	99	132	162	82	158	211	254	48	103	140	180	68	135	190	226	27	54	65	71
<i>C-RNN</i>	47	102	141	177	76	149	203	247	49	100	124	158	70	158	214	247	26	53	63	69
<i>C-RNN+OMP</i>	53	99	127	155	128	154	197	239	49	96	121	149	61	127	168	199	29	55	65	70
<i>C-RNN+LI</i>	43	89	117	142	72	141	188	230	47	92	117	147	72	145	194	219	27	53	63	69
<i>C-RNN+OMP+LI</i>	44	89	116	142	115	156	204	251	48	95	121	147	77	152	195	219	26	53	63	68

Object motion prediction	Passing objects				Grasping or leaving object				Cutting food				Mixing objects				Cooking			
Time (s)	0.5	1	1.5	2	0.5	1	1.5	2	0.5	1	1.5	2	0.5	1	1.5	2	0.5	1	1.5	2
ZV	48	118	181	237	65	152	226	289	29	70	104	132	50	126	188	229	16	33	44	53
RNN	49	107	154	198	64	139	201	257	29	70	105	134	47	113	166	199	17	36	48	58
<i>C-RNN+OMP</i>	44	92	122	150	55	103	136	167	31	64	83	97	29	65	90	110	15	33	46	56
<i>C-RNN+OMP+LI</i>	44	91	119	142	58	112	152	186	29	62.4	81	92	51	106	145	171	16	34	46	55

Table 2: **Class-specific models results.** In this table, every action is independently trained. The results report the mean Euclidean error (in mm), for the 2s prediction of the human motion (top) and object motion (bottom). In all cases, 1s of past observations is provided. The context-based models we propose in this paper are those with the suffixes “OMP” and “LI”. They provide the best results in most sequences.

All																				
Human motion prediction																				
Time (s)	0.1	0.2	0.3	0.4	0.5	0.6	0.7	0.8	0.9	1	1.1	1.2	1.3	1.4	1.5	1.6	1.7	1.8	1.9	2
ZV [34]	24	46	67	87	106	125	143	160	176	190	205	219	231	244	256	267	279	290	300	310
RNN [34]	29	44	57	68	78	87	96	104	113	121	128	136	143	150	157	164	171	177	184	191
<i>C-RNN</i>	27	46	58	69	79	87	96	104	113	121	129	137	144	152	160	166	174	181	188	196
<i>C-RNN+OMP</i>	46	83	76	82	87	95	101	108	116	123	131	138	146	153	160	167	174	182	189	197
<i>C-RNN+LI</i>	21	39	52	63	72	80	89	97	104	111	118	125	131	137	144	150	157	163	170	177
<i>C-RNN+OMP+LI</i>	39	77	77	76	80	87	94	101	108	114	120	126	133	139	145	151	158	165	171	178

All																				
Object motion prediction																				
Time (s)	0.1	0.2	0.3	0.4	0.5	0.6	0.7	0.8	0.9	1	1.1	1.2	1.3	1.4	1.5	1.6	1.7	1.8	1.9	2
ZV	13	25	35	44	52	60	68	77	84	90	96	102	109	115	120	125	131	135	140	144
RNN	15	28	38	46	53	60	68	74	80	85	91	97	102	107	112	117	121	125	130	135
<i>C-RNN+OMP</i>	15	26	36	44	50	55	61	67	73	79	84	89	94	99	104	108	113	117	121	125
<i>C-RNN+OMP+LI</i>	16	29	39	46	52	57	63	69	75	79	84	88	93	97	101	105	110	114	117	121

Table 3: **Training with all actions simultaneously.** For each method we train a single model using all actions simultaneously. See also caption in Table 2.

RNN. We also consider a Zero-Velocity (ZV) baseline that constantly predicts the last observed frame. Surprisingly, as we shall see later, this is a simple baseline that no other proposed method beats consistently. We consider the same two baselines for object motion prediction, where the position of an object is defined by its 3D bounding box.

It is worth mention that we also trained GAN-based models such as [12, 3, 40, 24] but their performance was significantly worse than models trained directly to minimize $L2$ distance.

Our models. We run our context-aware models (*C-RNN*), incrementally adding the main ideas described in the paper.

The basic *C-RNN* in our experiments uses the spatial heuristic described in Section 4.2 where interactions depend only on the distance between objects. This model processes context during the past frames, and then uses the last hidden state of the human node for human motion prediction at each step. This is extended by additionally predicting object motion (*OMP*) and recompute object interaction using the previous assumption on the predicted positions.

We then evaluate the efficiency of our model for learning interactions (*LI*). Like in the previously defined experiments, we evaluate a model that considers past contextual information and a model that prolongs object analysis into the future.

Evaluation metric. Since recent works on human motion prediction compute relative motion [34, 12], their evaluation metric is based on mean angle errors. In this paper, however, we are able to predict absolute motion. Therefore we use the mean Euclidean Distance (in mm) between the predictions and the real future motion, obtained from the unnormalized predictions in the 3D space. For human motion prediction, we take into account the 18 joints defined in the human skeleton. For objects, we consider the 8 3D vertices of their bounding boxes.

Quantitative results. Table 2 summarizes the performance of class-specific models trained on different activities. Table 3 provides results at much higher temporal resolution for models trained using all the dataset, reporting the mean Eu-

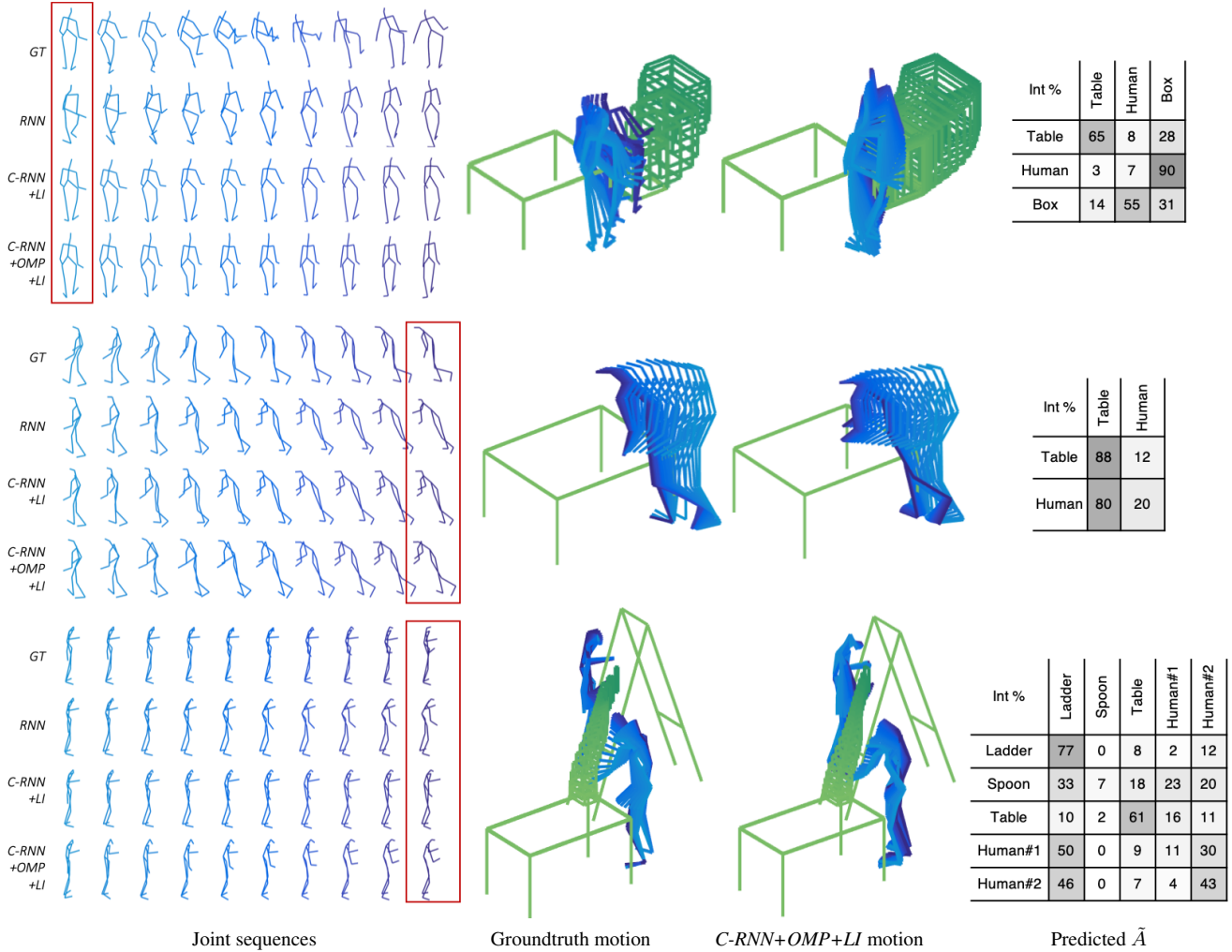


Figure 3: **Qualitative motion generation up to two seconds.** **Left:** Predicted sample frames of our approaches and the baselines. **Center:** Detail of the predictions obtained with our approaches, compared with the ground truth. Human and object motion are represented from light blue to dark blue and light green to dark green, respectively. Actions, from top to bottom are: A human supports on a table to kick a box, human leaning on a table, and two people (one of them standing on a ladder) passing an object. **Right:** Predicted adjacency matrices representing the interactions learned by our model. Note that these relations are directional (e.g. in the last example the ladder highly influences the motion of the Human#1 (50%) but the human has very little influence over the ladder (11%). Best viewed in color with zoom.

clidean distance between predictions and ground truth every 100 ms. In all cases, 1 second of past observations is provided and 2 seconds are predicted.

The performance of models that consider a threshold-based binary interaction vary significantly between classes, suggesting they are effectively unable to understand the context as done by models that learn the actual interactions (*LI*). Notice that even the basic *C-RNN* does not yet provide a consistent improvement compared to state-of-art models. The same model that additionally learns interactions (*C-RNN+LI*) does obtain a significant boost in most cases. Nonetheless, activities such as passing objects or

grasping require attending to items that are at variable distances.

Regarding the complexity of the scene, most improvement comes from scenes with a small number of objects where interactions are well defined and actions are more predictable. For cooking activities, there are several objects in a table next to the human. Different motion options are possible and, as uncertainty grows, the model seems unable to confidently understand interactions. Because of this, context-aware models do not provide such a significant improvement as in previous activities.

Considering all actions simultaneously seems to fa-

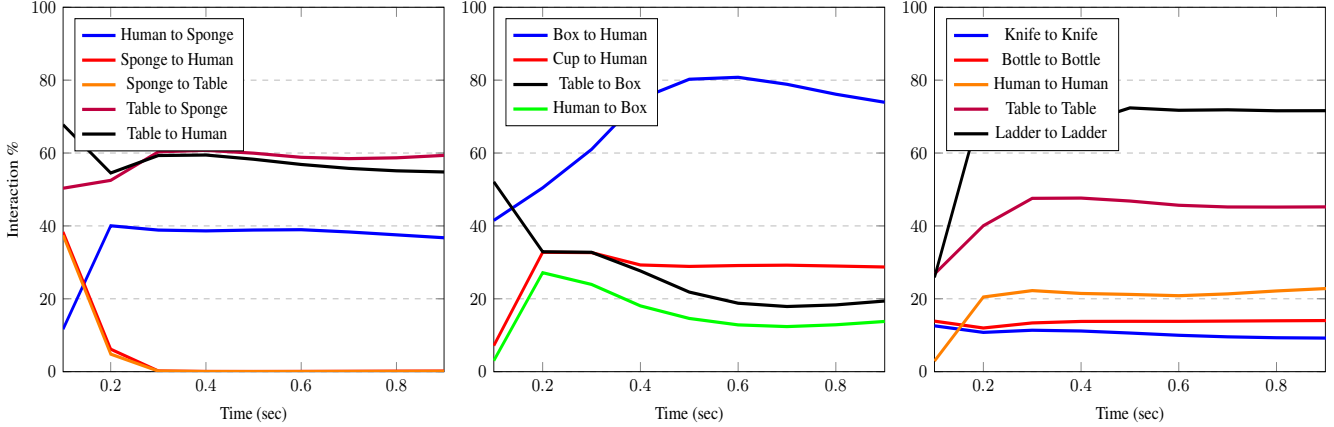


Figure 4: **Average interactions refined by the model during the past observations of the context.** In the left and center plots, we depict relevant interactions for *table cleaning* and *moving box* activities respectively. In the first case, notice the table affects significantly the sponge and human, which initially moves towards the table to clean it. Similarly, in the second case, the human moves towards a box on the ground, picks it up and puts it on the table. The right plot shows average self-interaction percentages among all the test samples, for relevant object types. We found that non-moving objects like tables or ladders consistently have very little influence from other objects. Likewise, passive objects that are often moved by a human, such as knives or bottles, are more influenced by them and leave self-influence relatively low.

vor even more the context-aware approaches and, specially, those that learn interactions (*C-RNN+LI* and *C-RNN+OPM+LI*).

Qualitative results. Figure 3-left shows the motion generation results of our two main models, compared to the baseline [34] on different classes. We did not include the Zero-Velocity baseline as it does not provide interesting motion even though it has remained a difficult baseline on uncertain activities. We have marked some specific frames in which context-aware approaches improve the RNN baseline.

For human motion prediction, poses generated are frequently more semantically-related to their closest objects than context-less models. For instance, as shown in the last action of Figure 3, people holding objects tend to move the relevant hand. For object motion prediction, context-less model predictions hardly move from their original position.

Regarding the interactions predicted by the model, we notice coherent patterns in many activities. For example, drinking videos generate strong Cup-Human relationships. In Figure 4, we represent the average predicted interactions for different actions. These are gathered from the *C-RNN+OPM+LI*. This model provides more intense Object-Object interactions than *C-RNN+LI*, which does not need to obtain such meaningful representations for objects as only human contextual representations are used. Note that the models learn to predict interactions that provide information relevant to future pose, and thus improve motion predictions. Interactions here do not necessarily respond to actual action relationships.

7. Conclusion

In this work, we explore a context-aware motion prediction architecture, using a semantic-graph representation where objects and humans are represented by nodes independently of the number of objects or complexity of the environment. We extensively analyze their contribution for human motion prediction. The results observed in different actions suggest that the models proposed are able to understand human activities performed significantly better than state-of-art models which do not use context, improving both human and object motion prediction. In particular, we notice clear improvements in activities well defined by the context, such as people handing objects or grasping items from a table.

We additionally extend the classical human motion prediction setting and propose to consider motion for all objects in a scene simultaneously. Despite adding a new task and loss function for these new models, without increasing their capacity, they obtain comparable results in the human motion prediction task. In object motion prediction, consistent improvements show that context-awareness is even more decisive, as objects are passive entities moved only through human actions.

Among the results provided in this work, we find that coherent predicted interactions are particularly encouraging for further work on unsupervised context understanding. Additional future work may focus on context-conditional motion generation.

Acknowledgements: This work is supported in part by an

Amazon Research Award, by the Spanish Ministry of Science and Innovation under projects HuMoUR TIN2017-90086-R, ColRobTransp DPI2016-78957 and María de Maeztu Seal of Excellence MDM-2016-0656. We also thank Nvidia for hardware donation.

References

- [1] F. Althché and A. de La Fortelle. An lstm network for highway trajectory prediction. In *ITSC*, pages 353–359. IEEE, 2017. **2**
- [2] M. Arjovsky, S. Chintala, and L. Bottou. Wasserstein gan. *arXiv preprint arXiv:1701.07875*, 2017. **2**
- [3] E. Barsoum, J. Kender, and Z. Liu. Hp-gan: Probabilistic 3d human motion prediction via gan. In *Proceedings of the IEEE Conference on Computer Vision and Pattern Recognition Workshops*, pages 1418–1427, 2018. **1, 2, 5, 6**
- [4] W. Byeon, Q. Wang, R. Kumar Srivastava, and P. Koumoutsakos. Contextvp: Fully context-aware video prediction. In *ECCV*, pages 753–769, 2018. **2**
- [5] Y. Chen, M. Rohrbach, Z. Yan, S. Yan, J. Feng, and Y. Kalantidis. Graph-based global reasoning networks. *arXiv preprint arXiv:1811.12814*, 2018. **1, 3**
- [6] K. Cho, B. Van Merriënboer, D. Bahdanau, and Y. Bengio. On the properties of neural machine translation: Encoder-decoder approaches. *arXiv preprint arXiv:1409.1259*, 2014. **5**
- [7] N. Deo, A. Rangesh, and M. M. Trivedi. How would surround vehicles move? a unified framework for maneuver classification and motion prediction. *Intelligent Vehicles (IV)*, 3(2):129–140, 2018. **2**
- [8] K. Fragkiadaki, S. Levine, P. Felsen, and J. Malik. Recurrent network models for human dynamics. In *ICCV*, pages 4346–4354, 2015. **1, 2**
- [9] P. Ghosh, J. Song, E. Aksan, and O. Hilliges. Learning human motion models for long-term predictions. In *2017 International Conference on 3D Vision (3DV)*, pages 458–466. IEEE, 2017. **1**
- [10] G. Gkioxari, R. Girshick, and J. Malik. Actions and attributes from wholes and parts. In *Proceedings of the IEEE International Conference on Computer Vision*, pages 2470–2478, 2015. **2**
- [11] I. Goodfellow, J. Pouget-Abadie, M. Mirza, B. Xu, D. Warde-Farley, S. Ozair, A. Courville, and Y. Bengio. Generative adversarial nets. In *NIPS*, pages 2672–2680, 2014. **2**
- [12] L.-Y. Gui, Y.-X. Wang, X. Liang, and J. M. Moura. Adversarial geometry-aware human motion prediction. In *ECCV*, pages 786–803, 2018. **1, 2, 6**
- [13] K. He, X. Zhang, S. Ren, and J. Sun. Deep residual learning for image recognition. In *CVPR*, pages 770–778, 2016. **3**
- [14] R. Herzig, M. Raboh, G. Chechik, J. Berant, and A. Globerson. Mapping images to scene graphs with permutation-invariant structured prediction. In *NIPS*, pages 7211–7221, 2018. **2**
- [15] H. Hu, J. Gu, Z. Zhang, J. Dai, and Y. Wei. Relation networks for object detection. In *CVPR*, June 2018. **3**
- [16] C. Ionescu, D. Papava, V. Olaru, and C. Sminchisescu. Human3.6m: Large scale datasets and predictive methods for 3d human sensing in natural environments. *PAMI*, 36(7):1325–1339, 2014. **1, 2, 5**
- [17] A. Jain, A. R. Zamir, S. Savarese, and A. Saxena. Structural-rnn: Deep learning on spatio-temporal graphs. In *CVPR*, pages 5308–5317, 2016. **1, 2, 3**
- [18] D. P. Kingma and J. Ba. Adam: A method for stochastic optimization. *arXiv preprint arXiv:1412.6980*, 2014. **5**
- [19] T. N. Kipf and M. Welling. Semi-supervised classification with graph convolutional networks. *arXiv preprint arXiv:1609.02907*, 2016. **3, 4**
- [20] T. N. Kipf and M. Welling. Semi-supervised classification with graph convolutional networks. *ICLR*, 2016. **5**
- [21] H. S. Koppula, R. Gupta, and A. Saxena. Learning human activities and object affordances from rgb-d videos. *The International Journal of Robotics Research*, 32(8):951–970, 2013. **1, 2, 5**
- [22] H. S. Koppula and A. Saxena. Anticipating human activities using object affordances for reactive robotic response. *PAMI*, 38(1):14–29, 2016. **1**
- [23] L. Kovar, M. Gleicher, and F. Pighin. Motion graphs. In *ACM SIGGRAPH 2008 classes*, page 51. ACM, 2008. **1**
- [24] J. N. Kundu, M. Gor, and R. V. Babu. Bihmp-gan: Bidirectional 3d human motion prediction gan. *arXiv preprint arXiv:1812.02591*, 2018. **2, 6**
- [25] C. G. Lab. Cmu motion capture database. <http://mocap.cs.cmu.edu/>. **1, 5**
- [26] C. Lea, A. Reiter, R. Vidal, and G. D. Hager. Segmental spatiotemporal cnns for fine-grained action segmentation. In *ECCV*, pages 36–52. Springer, 2016. **3**
- [27] R. Li, M. Tapaswi, R. Liao, J. Jia, R. Urtasun, and S. Fidler. Situation recognition with graph neural networks. In *Proceedings of the IEEE International Conference on Computer Vision*, pages 4173–4182, 2017. **2**
- [28] Y.-L. Li, S. Zhou, X. Huang, L. Xu, Z. Ma, H.-S. Fang, Y.-F. Wang, and C. Lu. Transferable interactiveness prior for human-object interaction detection. *arXiv preprint arXiv:1811.08264*, 2018. **1, 2**
- [29] Y. Liu, R. Wang, S. Shan, and X. Chen. Structure inference net: object detection using scene-level context and instance-level relationships. In *CVPR*, pages 6985–6994, 2018. **3**
- [30] W. Luo, B. Yang, and R. Urtasun. Fast and furious: Real time end-to-end 3d detection, tracking and motion forecasting with a single convolutional net. In *CVPR*, pages 3569–3577, 2018. **2**
- [31] Z. Luo, B. Peng, D.-A. Huang, A. Alahi, and L. Fei-Fei. Unsupervised learning of long-term motion dynamics for videos. In *CVPR*, pages 2203–2212, 2017. **2**
- [32] C.-Y. Ma, A. Kadav, I. Melvin, Z. Kira, G. AlRegib, and H. Peter Graf. Attend and interact: Higher-order object interactions for video understanding. In *CVPR*, pages 6790–6800, 2018. **2**
- [33] C. Mandery, Ö. Terlemez, M. Do, N. Vahrenkamp, and T. Asfour. The kit whole-body human motion database. In *ICAR*, pages 329–336. IEEE, 2015. **5**

- [34] J. Martinez, M. J. Black, and J. Romero. On human motion prediction using recurrent neural networks. In *CVPR*, pages 2891–2900, 2017. [1](#), [2](#), [3](#), [4](#), [5](#), [6](#), [8](#)
- [35] A. Newell and J. Deng. Pixels to graphs by associative embedding. In *NIPS*, pages 2171–2180, 2017. [2](#)
- [36] B. Ni, X. Yang, and S. Gao. Progressively parsing interactional objects for fine grained action detection. In *CVPR*, pages 1020–1028, 2016. [3](#)
- [37] B. Paden, M. Čáp, S. Z. Yong, D. Yershov, and E. Frazzoli. A survey of motion planning and control techniques for self-driving urban vehicles. *Intelligent Vehicles (IV)*, 1(1):33–55, 2016. [1](#)
- [38] S. Parisot, S. I. Ktena, E. Ferrante, M. Lee, R. Guerrero, B. Glocker, and D. Rueckert. Disease prediction using graph convolutional networks: Application to autism spectrum disorder and alzheimer’s disease. *Medical image analysis*, 48:117–130, 2018. [3](#)
- [39] S. Qi, W. Wang, B. Jia, J. Shen, and S.-C. Zhu. Learning human-object interactions by graph parsing neural networks. In *ECCV*, pages 401–417, 2018. [2](#), [3](#), [5](#)
- [40] A. H. Ruiz, J. Gall, and F. Moreno-Noguer. Human motion prediction via spatio-temporal inpainting. *arXiv preprint arXiv:1812.05478*, 2018. [2](#), [6](#)
- [41] P. Veličković, G. Cucurull, A. Casanova, A. Romero, P. Lio, and Y. Bengio. Graph attention networks. *arXiv preprint arXiv:1710.10903*, 2017. [4](#)
- [42] J. Walker, A. Gupta, and M. Hebert. Dense optical flow prediction from a static image. In *ICCV*, pages 2443–2451, 2015. [2](#)
- [43] X. Wang and A. Gupta. Videos as space-time region graphs. In *ECCV*, pages 399–417, 2018. [3](#), [4](#)
- [44] Y. Wang, Y. Sun, Z. Liu, S. E. Sarma, M. M. Bronstein, and J. M. Solomon. Dynamic graph cnn for learning on point clouds. *arXiv preprint arXiv:1801.07829*, 2018. [3](#), [4](#), [5](#)
- [45] M. Yatskar, L. Zettlemoyer, and A. Farhadi. Situation recognition: Visual semantic role labeling for image understanding. In *CVPR*, pages 5534–5542, 2016. [2](#)